Available online at www.sciencedirect.com
SCIENCE DIRECT®
PERGAMON
International Journal of Multiphase Flow 29 (2003) 527–558
International Journal of Multiphase Flow
www.elsevier.com/locate/ijmulflow

Experimental study of two and three phase flows in large diameter inclined pipes

G. Oddie [a,*], H. Shi [b], L.J. Durlofsky [b,c], K. Aziz [b], B. Pfeffer [a], J.A. Holmes [d]

[a] *Schlumberger Cambridge Research, High Cross, Madingley Road, Cambridge, CB3 0EL, UK*
[b] *Department of Petroleum Engineering, Stanford University, Stanford, CA 94305, USA*
[c] *ChevronTexaco EPTC, San Ramon, CA 94583, USA*
[d] *Schlumberger GeoQuest, 11 Foxcombe Court, Wyndyke Furlong, Abingdon, Oxfordshire, OX14 1DZ, UK*

Received 29 April 2002; received in revised form 13 January 2003

Abstract

Steady-state and transient experiments of water–gas, oil–water and oil–water–gas multiphase flows were conducted on a transparent 11 m long, 15 cm diameter, inclinable pipe using kerosene, tap water and nitrogen. The pipe inclination was varied from 0° (vertical) to 92° and the flow rates of each phase were varied over wide ranges. Fast-acting valves enabled the trapping of the fluid flowing in the pipe, which in turn allowed for the accurate measurement of the absolute volumetric fraction (holdup) of each phase. A nuclear densitometer, as well as ten electrical probes at various locations along the pipe, provided additional steady-state and transient measurements of the holdup. A total of 444 tests were conducted, including a number of repeated tests. Bubble, churn, elongated-bubble, slug, and stratified/stratified-wavy flows were observed for water–gas and oil–water–gas flows, while dispersed/homogeneous, mixed/semi-mixed and segregated/semi-segregated flows were observed for oil–water flows. Extensive results for holdup as a function of flow rates, flow pattern and pipe inclination are reported, and the various techniques for measuring holdup are compared and discussed. The flow pattern and shut-in holdup are also compared with the predictions of a mechanistic model. Results show close agreement between observed and predicted flow pattern, and a reasonable level of agreement in holdup.

Keywords: Two phase; Three phase; Large diameter; Inclined; Steady-state; Transient; Water–gas; Oil–water; Oil–water–gas; Wellbore; Holdup; Flow pattern; Mechanistic model

* Corresponding author.
E-mail address: oddie@cambridge.oilfield.slb.com (G. Oddie).

0301-9322/03/$ - see front matter
doi:10.1016/S0301-9322(03)00015-6

1. Introduction

The accurate modeling of fluid flow in subsurface formations is essential for the proper management of petroleum reservoirs. Reservoir simulators, which model the flow and transport of reservoir fluids (oil, water and gas), are commonly applied for this purpose. Within the reservoir simulator, it is important to accurately represent the interaction of the reservoir with the wellbore. This modeling is complicated because of wellbore hydraulics, which can impact the flow from the reservoir into the wellbore. In the case of long horizontal or deviated wells, the effect of pressure losses within the wellbore can be very significant and can lead to a number of deleterious effects (Dikken, 1990), such as the premature coning of unwanted water or gas or the loss of production at the far end (toe) of the well. In order to predict and thereby mitigate these effects, it is essential that accurate models for multiphase wellbore flow be included in reservoir flow simulators.

Many of the available simulators do include models for multiphase flow in the wellbore. In one such implementation, the wellbore is divided into a number of segments and a drift-flux model is then applied to model two and three phase flows (Holmes et al., 1998). This and other such models typically combine different published experimental and theoretical correlations to determine the drift-flux model parameters. While the results from these models often appear to be reasonable, the experiments from which the correlations were developed were mostly performed for two phase flows in small diameter ($\leqslant \sim 5$ cm) pipes. Wellbores, by contrast, are typically of diameter 8–25 cm. This size discrepancy can be important, as it has been observed that the flow mechanisms in small pipes may be significantly different from those of larger pipes. For example, Jepson and Taylor (1993) claimed that only pipes of diameter 7.5 cm and greater can mimic the mechanisms observed in large diameter pipelines. In addition, most previous experimental studies were for horizontal or vertical pipes, although it is known that flow pattern, phase distribution and pressure drop can be greatly affected by the inclination. Therefore, it is very important to test and validate the existing models, and to develop new models through incorporation of data from large diameter, inclined pipes.

The widespread occurrence of multiphase flow in pipes has prompted extensive research in this area. However, there is still a lack of adequate large diameter, inclined pipe, multiphase flow data. Our ultimate goal in this work is to validate and, where necessary, extend current wellbore flow models. The first stage of this work, which we describe in this paper, is to perform a series of suitably designed multiphase flow tests in a well-instrumented, large-scale experimental apparatus. The data must be of sufficient quality and quantity to be of practical use and to support the development of new models.

In this work we study two phase liquid–gas (water–nitrogen) flow, liquid–liquid (kerosene–water) flow, and three phase liquid–gas (kerosene–water–nitrogen) flow. Considerable research has been focused on two phase liquid–gas flow in horizontal and vertical pipes, though much less work has been reported for two phase oil–water flow and three phase oil–water–gas flow. We now discuss previous work in these areas, with emphasis on results for large diameter (>7.5 cm) pipes.

Scott et al. (1989) collected field data on large diameter (30–61 cm) flow lines at Prudhoe Bay for a slug flow study. They instrumented the pipe with nuclear densitometers, flow meters, and pressure and temperature sensors. Scott et al. modified an existing slug-length correlation to match these large diameter data. Gopal and Jepson (1997) developed a nonintrusive flow visualization method for the quantitative study of slug flow in a 7.5 cm diameter, 10 m long, hori-

zontal plexiglass pipe. Slugs were recorded on video and void fraction profiles were then determined by image analysis. A dynamic model was developed to predict the variation of the average liquid holdup within the slug. Cheng et al. (2000) studied liquid–gas flow in a 15 cm diameter, 10.5 m high vertical column. They found that traditional slug flow, as would be observed in smaller diameter pipes under these conditions, did not exist in this system. Instead, they observed a gradual transition to churn flow. A similar observation was also made by Ohnuki and Akimoto (2000), who studied water–air vertical flow in a 20 cm diameter pipe. They also observed that churn flow is dominant in large diameter vertical pipes under the conditions where small diameter pipes exhibit slug flow.

Studies on two phase flow in inclined pipes have been performed in the past, though most of this work involved small diameter pipes. The work of Beggs (1972) and Beggs and Brill (1973), who studied inclined liquid–gas flow in small diameter pipes, has been widely applied in the petroleum industry. This work provides empirical correlations for the prediction of holdup and pressure drop. Hasan and Kabir (1988) conducted experiments in a 12.5 cm pipe and annular flow channels with inner tube diameters of 4.8, 5.7 and 8.7 cm for deviations up to 32° from vertical. These experiments, performed at very low water flow rates, were conducted by feeding air into a stagnant water column. The model developed by Hasan and Kabir (1988) performs about as well as the Beggs and Brill (1973) model.

A more recent study of two phase flow in small diameter inclined pipes was conducted by Tshuva et al. (1999). These researchers studied upward water–air flows at a number of different inclinations in 2.4 cm diameter, 3 m long pipes. It was found that the flow distribution can be either symmetric or asymmetric depending on the flow conditions and pipe inclination. A model was proposed to explain the observed phenomena. To examine the effect of small downward inclinations on the formation of slugs, Woods et al. (2000) conducted water–air experiments in a 7.6 cm diameter, 23 m long pipe with inclinations of −0.2°, −0.5°, and −0.8° from horizontal. They observed significant differences in the flow for these slightly inclined pipes relative to horizontal systems.

The flow characteristics of oil–water mixtures are generally different from liquid–gas systems, so the results of liquid–gas flow cannot be applied directly to oil–water flow in most cases. In oil–water flow, the formation of emulsions, which requires a proper calculation of emulsion viscosity, and phase inversion, which causes a sudden increase or decrease in pressure drop and mixture viscosity, make the problem even more complicated (Arirachakaran et al., 1989; Shi, 2001). Furthermore, drag reduction, in which the more viscous phase is dispersed in the less viscous phase, thus causing a reduction in pressure gradient, was observed by Pal (1993) and Angeli and Hewitt (1998) for turbulent flows. Angeli and Hewitt (1998) also found that oil–water flow behaves differently depending on the tube wall material. In the case of three phase flow, even the flow patterns are in general extremely complicated (Açikgöz et al., 1992; Lahey et al., 1992; Lee, 1993; Wu et al., 2001), and no validated engineering models for wellbore flow currently exist.

Extensive two phase experiments were conducted by Ouyang et al. (1998) in 11 and 15.5 cm diameter pipes. Most of their data are for flow in horizontal and nearly horizontal pipes with radial influx along the pipe. The data were used to quantify the effect of inflow on single and two phase friction factors.

While most studies for inclined two phase flow have been concerned with liquid–gas systems, there have been some studies involving oil–water flows. In recent work, Flores et al. (1997) studied

oil–water flow experimentally and theoretically in vertical and inclined 5 cm pipes. They observed water holdup to be strongly affected by flow pattern and inclination and proposed a mechanistic model to predict holdup in vertical wells. They found that a homogeneous model was adequate for flow patterns showing negligible slippage and a drift-flux approach gave reasonable results for the high slippage flow patterns. Holdup and velocity profiles of oil–water flows in 10 cm diameter inclined pipes were investigated by Vedapuri (1999). The experiments were performed at six different inclinations ($\pm 2°$, $\pm 5°$, $\pm 15°$). Inclination was found to affect both holdup and velocity profiles.

Very little data are available for three phase flows in large diameter, inclined pipe, and most of the few reported studies are only flow pattern investigations. Along these lines, Wilkens (1997) investigated the flow regime transitions and the effects of inclination, pressure, and water cut for a light oil–saltwater–carbon dioxide system. The experiments were carried out on an 18 m long, 10 cm diameter, high-pressure (13 MPa), high temperature (90 °C), inclinable stainless steel flow-loop at inclinations of 0°, $\pm 2°$ and $\pm 5°$ from horizontal. A mechanistic model was developed to predict the flow regime transitions. In the petroleum industry, oil–water–gas flow is often treated as a type of liquid–gas flow. However, the conditions under which such a treatment is justified have not been established. More experimental measurements are clearly required for the development of improved models for three phase flow in large diameter inclined systems.

The experimental data presented in this study fill some of the gaps identified above. We measure the flow of water–nitrogen, kerosene–water, and kerosene–water–nitrogen, at different flow rates and at eight deviations covering the range from vertical to 2° downward in a 15 cm diameter pipe. Results for steady-state and transient flows are reported. Both shut-in (final state after valve closure) and nuclear measurements are applied for the determination of steady-state holdup. Electrical probe data additionally provide an estimate of holdup as a function of axial position both in steady-state and during the transient after shut-in. The accuracy of these various measurements is discussed and assessed.

We then provide extensive results for flow pattern and steady-state holdup as a function of phase flow rates and pipe inclination. The observed flow patterns and holdup data are compared with predictions from the Petalas and Aziz (2000) mechanistic model. Although based mostly on data from small diameter pipes, this model predicts flow pattern accurately. Holdup predictions are less accurate but are still generally reasonable. The results presented here, and the flow models we plan to develop based on these data, should enable the more accurate modeling of multiphase wellbore flow and the improved simulation of petroleum reservoir performance.

2. Experimental setup

2.1. Inclinable flow system

The experiments reported in this paper were performed at Schlumberger Cambridge Research (SCR). The SCR large inclinable flow-loop basically consists of the pipework represented in Fig. 1. The pipework is fixed to a table which can be deviated from 0° (upwards vertical) to 92° (slightly downhill). Therefore, the entire range of uphill flows can be investigated in the test section.

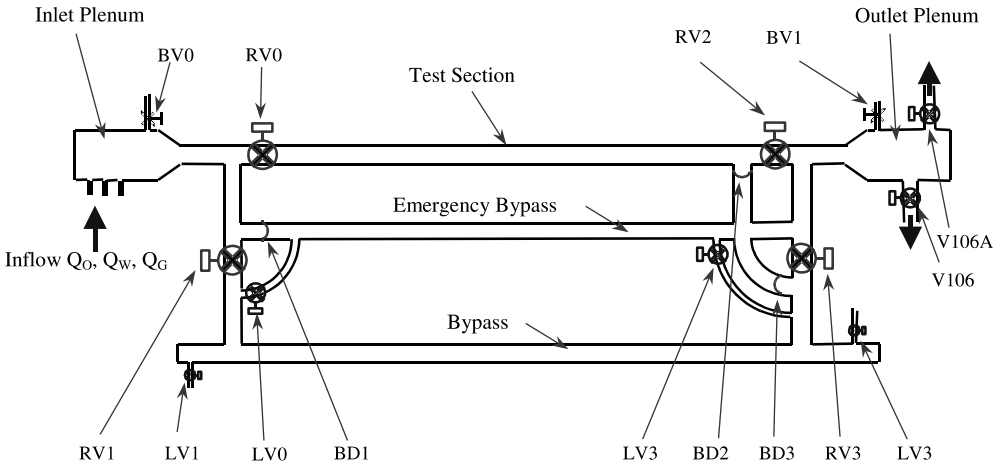

Fig. 1. Schematic of the pipework on the flow-loop table.

The main pipe, and also the test section, is a 10.9 m long and 15.2 cm diameter plexiglass pipe. At steady-state, oil, water and gas enter the pipework through an inlet plenum chamber, then flow along the test section, and finally leave the outlet plenum chamber through valves V106 for downward and horizontal flows or V106A for upward flows.

A bypass and four pneumatic rapid closing valves (RV0–RV3) were implemented to switch the flow between the test section and the bypass for transient flow tests. In the steady-state, RV0 and RV2 are open and allow the fluid to flow along the test section, while RV1 and RV3 stay closed in order to block the bypass so that it remains full of air. The air increases the compressibility of the system and minimizes the mass in the bypass that must be accelerated from rest at the beginning of the transient test. A transient test is carried out by shutting-in the test section. Within 100 ms, RV0 and RV2 close, and RV1 and RV3 open simultaneously. The error in the synchronization of these valves is less than about 20 ms, which results in errors in holdup of less than 1% at the highest flow rates. In the test section, the fluid is trapped almost instantaneously. Water hammer is reduced by diverting the upstream flow through the bypass.

The blowdown valves (LV0–LV3) were used to purge water from the bypass prior to the tests, and the bleed valves (BV0 and BV1) were controlled manually to add or remove air to the test section as necessary. An emergency bypass was also built to protect the flow-loop in case of the failure of any valve or combination of valves, so that the pressure rating and integrity of the flow-loop would not be compromised. Under normal circumstances, the bursting discs (BD1, BD2 and BD3) block the emergency bypass and prevent fluid from entering. They are designed to fail at 6 ± 1.5 bar, well below the flow-loop pressure limit of 10 bar.

2.2. Separator and pumps

Both water (tap water) and oil (kerosene with a viscosity of 1.5 cP at 18 °C and a density of 810 kg/m^3) were kept in the same large separator. Because of the difference in density, oil lies in the upper part of the vessel while water remains in the lower part. Two series of pipes, pumps,

flowmeters and hoses were used to transport separately the pure oil and pure water from the separator to the inlet chamber. A separate tank contains liquid nitrogen and supplies gas to the pipework. This tank contains evaporators and heat exchangers to bring the nitrogen to ambient temperature.

At the outlet of the flow-loop, a hose carries the combined fluid back to the separator. Gas reaches the top of the separator and escapes through a chimney, while the oil and water liquid phases remain in the separator. The separator contains several coalescer cartridges to accelerate the segregation of the three phases.

2.3. Flow-loop instrumentation

The instrumentation used in these experiments provides two types of data: (1) the reference measurements of flow, deviation, pressure and temperature and (2) the detailed measurements required to determine the flow distribution. The instrumentation installed along the test section is indicated in Fig. 2. The flow-loop is fitted with various reference measurements, which include:

- *Water rate*. Three electromagnetic flowmeters for water flow rate measurement.
- *Oil rate*. Three turbine flowmeters for oil flow rate measurement.
- *Gas rate*. Two thermal mass flowmeters for gas flow rate measurement.
- *Deviation*. Digital encoder on table bearings, 0–90° and 70°–92°.
- *Temperature*. Resistance thermometer 0–100 °C.
- *Flow-loop pressure*. Differential pressure diaphragm gauge, one arm open to atmosphere, −1.5 to +1.5 bar.
- *Differential pressure*. Differential pressure diaphragm gauge, same sensor as above.
- *Atmospheric pressure*. Absolute pressure gauge.

The other measurements are more specialized and include:

- *Video*. Two cameras are fixed to the flow-loop and allow us to record the flows from two visual angles, general overview and close-up.
- *Shut-in graduations*. The volume of the test section is marked in 2% increments along the length, with allowance made for the volume near the bursting disc (BD2). This allows an absolute measurement of the volumes of water, oil and gas to be made after shut-in to within less

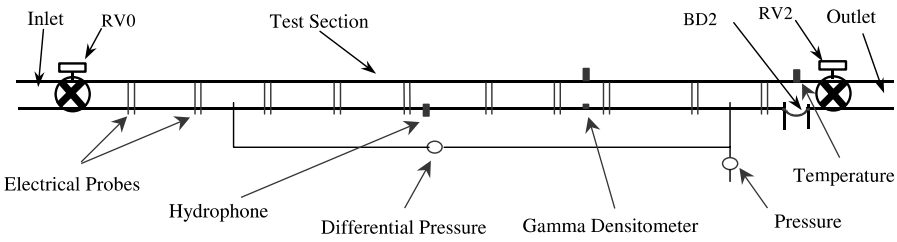

Fig. 2. Schematic of the test-section instrumentation.

than 1%. Due to the steel pipework near the outlet, holdups greater than 94% cannot be measured accurately.

- *Gamma densitometer*. A nuclear densitometer was installed 7.5 m from the inlet valve RV0. The gamma densitometer measures the gamma ray absorption, which allows the mean density of the fluid in the pipe to be calculated. The device was aligned on a vertical diameter with a 100 μ Ci Ba-133 source on the bottom of the pipe and the detector on the top. The data were gathered for five minutes giving typical counts of $N_W = 400{,}000$ when the pipe is filled with water, $N_O = 470{,}000$ when the pipe is filled with oil, and $N_G = 900{,}000$ when the pipe is filled with gas, where N designates the count. With these count rates, the measured density of a pure fluid in the path of the gamma ray beam can be estimated to 1% accuracy. The mean density of the in situ fluids (ρ_{exp}) is determined from the gamma densitometer count (N_{exp}) and the calibrations via the following equation (for water–gas systems):

$$\rho_{exp} = \rho_G + (\rho_W - \rho_G)\frac{\log(N_{exp}) - \log(N_G)}{\log(N_W) - \log(N_G)}. \tag{1}$$

The water holdup H_W (in situ fraction of water) is calculated by

$$H_W = \frac{\log(N_{exp}) - \log(N_G)}{\log(N_W) - \log(N_G)} = \frac{\rho_{exp} - \rho_G}{\rho_W - \rho_G}. \tag{2}$$

Expressions (1) and (2) are appropriate for homogeneous flow. For stratified flow, a geometric correction is introduced to account for the fact that the water lies near the pipe wall. The water holdup under the assumption of stratified flow (H_W^{strat}) is given by

$$H_W^{strat} = \frac{1}{\pi}(\cos^{-1}(1 - 2H_W) - (1 - 2H_W)\sin[\cos^{-1}(1 - 2H_W)]), \tag{3}$$

where H_W on the right-hand side of Eq. (3) is the homogeneous holdup computed from Eq. (2). The differences between H_W and H_W^{strat} are relatively slight for most values of holdup. The maximum absolute differences occur for $H_W = 19\%$ and 81%, where the $|H_W - H_W^{strat}| \sim 5.8\%$. The relative differences between H_W and H_W^{strat} are therefore the greatest at low values of holdup. This is consistent with our experimental observations (see Section 5.2.3).

A third approach for estimating holdup from N_{exp} is to assume that the fluid is in pure slug flow. By this we mean that slugs of 100% liquid are followed by zones of 100% gas. The relative sizes of these two zones define the holdup. In this case, holdup (H_W^{slug}) is given by

$$H_W^{slug} = \frac{N_{exp} - N_G}{N_W - N_G}. \tag{4}$$

In our presentation of results below, we will compare the holdup predictions of Eqs. (2)–(4) in order to gauge the magnitude of the error in the interpretation of the nuclear measurements.

For two phase flows, the holdup can be computed directly from the counts or the density as described above. For three phase flow, however, this direct connection no longer exists. In order to compute liquid holdup for these cases, we treat oil and water as one liquid phase. The nuclear count and the density of the oil–water mixture are calculated based on the input volume fraction. Thus, the slip between oil and water is assumed to be zero for these calculations.

- *Electrical probes*. Ten electrical conductivity probes, regularly spaced along the pipe, are used to measure the water depth. Each probe is comprised of two parallel brass rods (3 mm diameter, spaced 10 mm apart) which are fixed along the pipe diameter. The measurement of the resistance between the wires allows for the determination of the instantaneous water level around the probe. For stratified flows, the depth (h) at that location is easily measured. For more complex (e.g., dispersed) flows, an equivalent depth is derived from the signal.
- *Hydrophone*. Attached to the bottom of the pipe at 5.25 m to provide a backup for detecting the closure of the rapid valves or the failure of bursting discs.

2.4. Flow-loop control

Four independent computers were used to conduct the tests and to collect the data.

- A programmable logic controller enabled us to set the input water, oil and gas flow rates and to select the appropriate pumps and flowmeters.
- A second computer controlled the rapid-acting valves and triggered the shut-in of the flow-loop.
- For each test, the data acquisition system collected all of the relevant data (as described above) from the flow-loop. The signals from the electrical probes were low-pass filtered at 300 Hz and logged at 1 kHz. The valve trigger, valve position sensor and hydrophone were logged at 1 kHz and the remaining parameters were logged at 5 Hz.
- Another computer controlled the gamma-densitometer. It selected the acquisition parameters, triggered the nuclear count, and analyzed and stored the data.

2.5. Experimental procedure

At the beginning of each set of tests, and again at the end of the day, the electrical probes and gamma densitometer were calibrated. Starting with the test section filled with gas and deviated at 92° from vertical, water was allowed to enter at a constant rate. Signals from each of the probes were logged and the empty and full signals were used for calibration purposes. The calibration curve can also be used to identify problems such as poor wetting of the probes. The signal from the probes is nearly linear with depth. An additional correction to the calibration was applied during the data analysis stage, as discussed below. The loop was filled consecutively with gas, oil and then water and a nuclear count was taken for each phase. For two phase tests, the gamma densitometer calibrations for the two phases were used; for three phase tests, calibrations for the three phases were used under the assumption of no slip between the liquid phases.

Once the calibrations were completed, the flow conditions were specified and the flow was allowed to reach equilibrium (determined through observation of flow rates and video), at which time the data acquisition was started. Once the steady-state test was completed, the bypass was triggered, simultaneously shutting-in the test section and opening the bypass. The parameters continued to be logged as the fluids settled. After the end of the acquisition, the flow-loop was rotated to the vertical if necessary so that the final positions of the fluid interfaces could be measured directly from the markings on the test-section. This formed the transient test.

Table 1
Experimental test matrix

		Q_W (m^3/h)					
			2	10	40	100	
Water–gas flow	Q_G (m^3/h)	5	✓	✓	✓	✓	Q_G standard
$14 \times 8 = 112$ tests		20	✓	✓	✓	✓	condition
		50	✓	✓	✓		
		100	✓	✓	✓		
			2	10	40	100	130
Oil–water flow	Q_O (m^3/h)	2	✓	✓	Q_O/Q_W is too small to measure volumetric fraction		
$9 \times 8 = 72$ tests		10	✓	✓	✓	✓	✓
		40			✓	✓	
			2	10	40		
Oil–water–gas flow	Q_O (m^3/h)	2	✓	✓	✓	5	Q_G (m^3/h)
$7 \times 3 \times 8 = 168$ tests		10	✓	✓		10	
		40	✓	✓		50	

3. Test matrix

The general purpose of this experimental campaign was to collect a maximum amount of data on two and three phase flows in pipes. Therefore, it was necessary to plan several series of tests that would cover a wide range of flow rates for each phase, at different deviations, with a view to obtaining a number of flow patterns within the test section.

The test sequences for the water–gas, oil–water, and oil–water–gas experiments are shown in Table 1. Each combination of flow rates (Q_O, Q_W, Q_G) was repeated at each of the following eight deviations: 92°, 90°, 88°, 80°, 70°, 45°, 5° and 0° from upward vertical. These test matrices were devised to take optimum advantage of the flow-loop while respecting the limitations that $Q_O + Q_W + Q_G \leqslant 140$ m^3/h (necessary to allow the three phases enough time to settle in the separator) and $Q_O \leqslant Q_W + 25$ m^3/h (in order to allow enough time for oil and water to separate). Note that the total number of tests indicated in the tables is 352. An additional 92 tests were repeated, so the total number of tests conducted was 444.

4. Sample data results

Figs. 3–6 display some typical data plots. Each figure corresponds to the probe responses for a particular set of Q_O, Q_W and Q_G (as indicated). The results are plotted in terms of the dimensionless water depth (h/D) across a vertical diameter with 0 being the bottom of the pipe and 1 the top of the pipe. The probe responses are each plotted in different colors, as indicated in the figures. Holdup values (discussed in detail below) are measured at the end of the transient after shut-in. Note that the Q_G values do not exactly correspond to the values given in Table 1. This is because

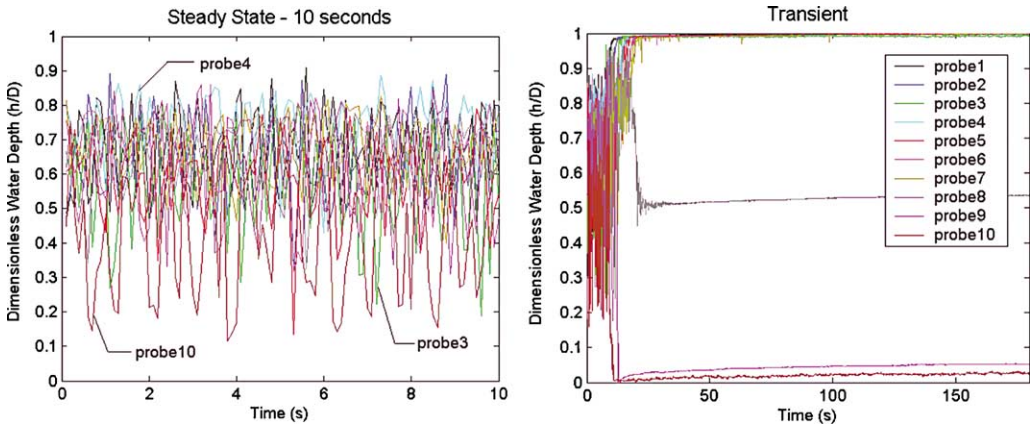

Fig. 3. Water–gas data for $\theta = 45°$, $Q_W = 40.4$ m^3/h, $Q_G = 62.8$ m^3/h ($H_W = 69\%$).

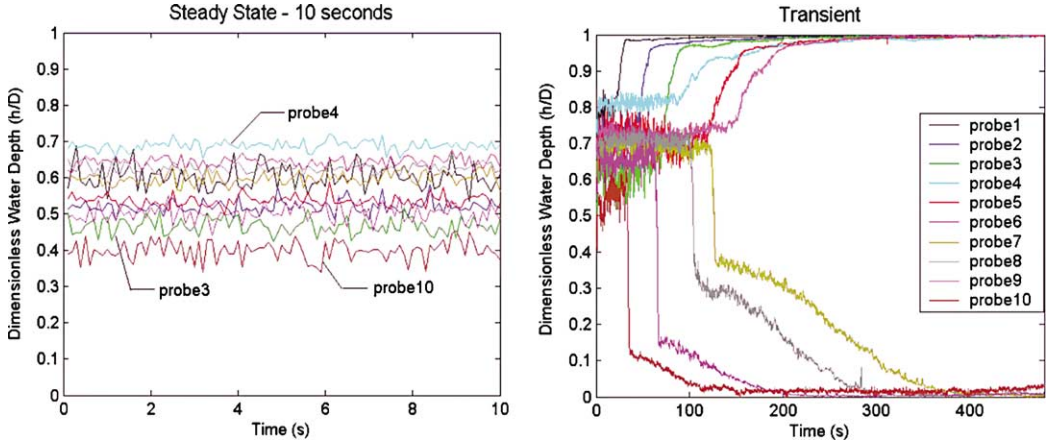

Fig. 4. Oil–water data for $\theta = 0°$, $Q_O = 10.0$ m^3/h, $Q_W = 10.1$ m^3/h ($H_W = 60\%$).

the values in Table 1 are target values at standard conditions, while the values cited here are actual (measured) values at flow-loop conditions.

The left figure in each of Figs. 3–6 is the steady-state plot. The variations of the water depth around the ten probes are plotted for a ten second interval. Though the probe responses clearly vary in time, the flow is steady in a statistical sense. Three of the probe responses are specifically indicated (probes 3, 4 and 10); these will be discussed below. A more detailed study of the probe data will allow us to estimate the speeds and the sizes of the gas bubbles, slug characteristics, etc. The graph on the right side displays the transient data (initial time here corresponds to shut-in). By focusing on the transient portion of the test, we can measure the settling time of the mixture. At the end of the transient, the phases are completely separated, with the probes located below the water interface totally immersed in water.

Though the probes were carefully calibrated, the transient data did not always show $h/D = 1$ for the probes that were fully immersed in water at the end of the transient period (e.g., probes 1–7

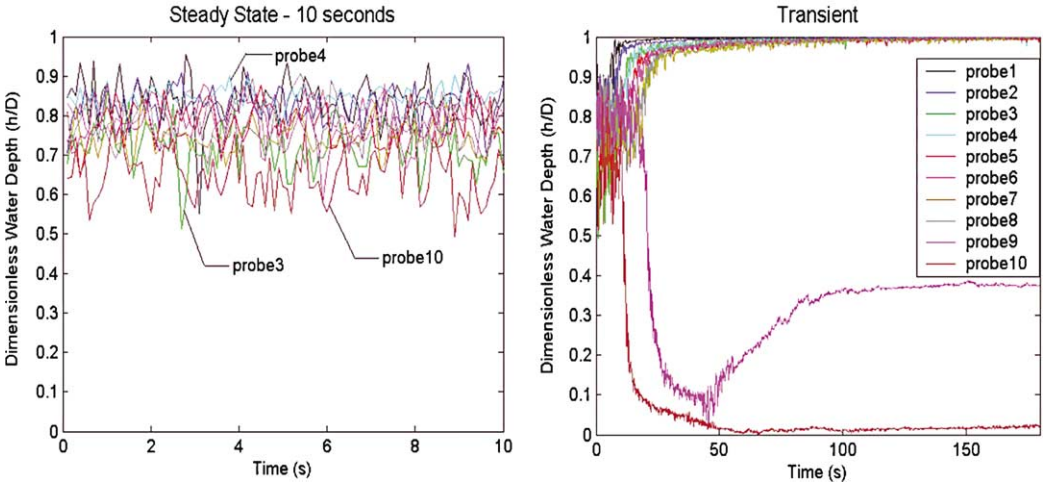

Fig. 5. Oil–water data for $\theta = 70°$, $Q_O = 10.0$ m^3/h, $Q_W = 10.1$ m^3/h ($H_W = 81\%$).

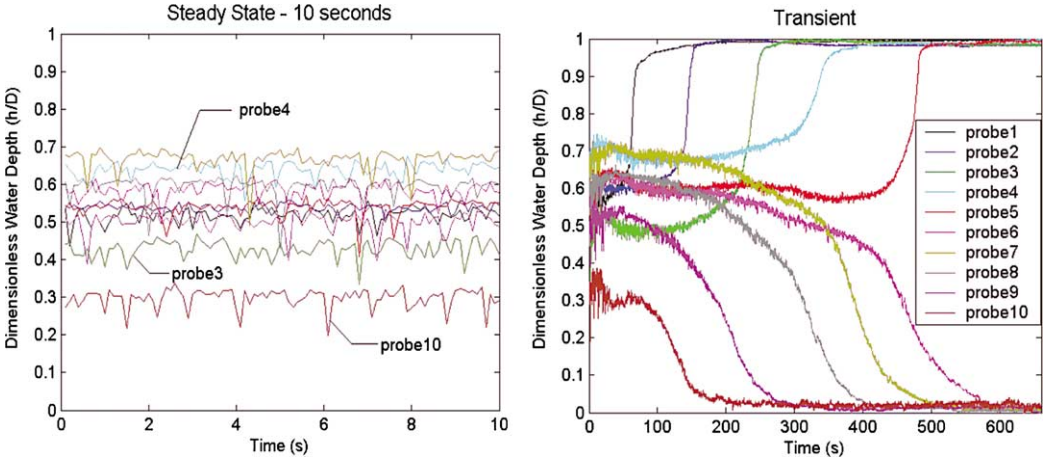

Fig. 6. Oil–water–gas data for $\theta = 0°$, $Q_O = 10.0$ m^3/h, $Q_W = 10.1$ m^3/h, $Q_G = 2.6$ m^3/h ($H_W = 50\%$, $H_O = 48\%$).

in Fig. 3). Similarly, probes fully immersed in oil or gas did not always register $h/D = 0$. Though these deviations were slight (typically less than 5%), we introduced an additional recalibration to eliminate most of this error. Specifically, if the probe ended the transient period fully immersed in water, we recalibrated it such that the maximum signal corresponded to $h/D = 1$. A similar treatment was introduced for probes fully immersed in oil or gas. This did not eliminate the probe endpoint errors entirely; see for example Fig. 3, where probes 9 and 10 still register nonzero h/D at the end of the transient even though they are fully immersed in gas. This occurs because the recalibration is based on the minimum signal, which occurred at a time of around 12 s.

Fig. 3 shows data for a high flow rate, water–gas test at a deviation of 45°. A churn flow was observed in this case. Most of the steady-state data tend to oscillate around $h/D \approx 0.6$–0.7 (note

that $H_W = 69\%$ in this case). The data from probe 10 (shown in brown) consistently fall below the data from the other probes, indicating a significant end effect. The end effect was most serious for the tests involving horizontal flows at low liquid holdup ($H_L < 40\%$) and downward flows, which suggests that the holdup results for these cases may display relatively large errors. This error will be further quantified in Section 5.2.2.

Data from probes 3 and 4 also vary somewhat from that of the other probes, though this variation is much less than that of probe 10. The probe 3 data is consistently below most of the other data (except for probe 10), while the probe 4 response tends toward the upper range of the data. The precise reason for this is unclear, but it does provide some indication of the accuracy of the probe data. We will see these effects more clearly below when we present the time-averaged axial holdup profiles.

From the transient profile in Fig. 3, probes 9 (purple) and 10 (orange) are observed to settle to zero depth (as expected) and probe 8 (shown in gray, at 7.75 m from the inlet or 70% holdup position when the pipe is vertical) is partially covered with water. This is consistent with the absolute measurement of water holdup of 69%. Note that the settling time for this experiment is very short (on the order of 10–20 s).

Fig. 4 shows the result of a vertical oil–water test at relatively low flow rates. A dispersed flow pattern was observed in this case. An interesting observation for the settling process of this oil–water mixture is that the probes near the midpoint of the pipe that are eventually covered by water reach their final state more quickly than the adjacent probes that are immersed in oil. This phenomenon, which was observed in a number of the tests, is likely due to several factors, including the position of the probes relative to the final interface and the fact that an oil-in-water emulsion separates faster than a water-in-oil emulsion. In addition, the probes detect an oil-in-water emulsion as pure water, so they do not register the change in holdup as this emulsion separates. In the future, we plan to model these effects in detail in order to develop quantitative descriptions of the transient separation process.

The next results, shown in Fig. 5, are for an oil–water system at the same flow rates as were considered previously, except now the pipe is deviated to 70° from the vertical (the pipe was vertical in the previous case). Dispersed flow was again observed. Comparison of Figs. 4 and 5 clearly shows that the settling time of the oil–water mixture is significantly reduced when the pipe is inclined. Specifically, in the vertical orientation settling required about 370 s; when $\theta = 70°$, the mixture settles in about 100 s. The transient signal for the $\theta = 70°$ case also displays some interesting behavior. Probe 9 (purple curve) first shows a decrease in water holdup (until about 50 s) but subsequently shows an increase in water holdup. A preliminary analysis suggests that this complex behavior is due to a phase inversion in this region of the pipe. We note finally that the water holdup increases from 60% for vertical flow to 81% at $\theta = 70°$, indicating that there is considerably more slippage between the two phases for higher pipe deviations. This finding will be shown more clearly below when we discuss the detailed results for holdup.

Fig. 6 displays results for a vertical oil–water–gas test. The water and oil flow rates are the same for this test as for the tests shown in Figs. 4 and 5. The flow pattern here was bubble flow. The relatively small amount of gas flow (less than 3 m^3/h) has a very large effect on the overall flow. Compared with the earlier oil–water vertical flow test (Fig. 4), the settling time is seen to be larger for the three phase flow case (nearly 600 versus 370 s). This is probably due to the extra mixing

caused by the gas motion through the mixture and the smaller droplet size of the discontinuous dispersed liquid phase.

5. Flow pattern and holdup

5.1. Flow pattern

The transparent test section allows for the observation of flow pattern. In this study, the basic flow patterns observed for oil–water–gas flows were also observed for liquid–gas two phase flows, although there are some differences, within the same flow pattern, between the two and three phase flows. Furthermore, although some of the flow patterns we observed in this large diameter, inclined pipe are not exactly the same as the classical flow patterns observed in small diameter vertical or horizontal pipes, we have tried to describe them in terms of the traditional flow pattern terminology rather than defining new flow patterns. An example of this will be given later.

Over the range of flow rates and pipe inclination angles considered here, bubble, churn, elongated-bubble, slug, stratified, and stratified wavy flow patterns were observed. All six of these flow patterns, as they were observed in actual experiments, are sketched in Fig. 7. The first four flow patterns, shown in Fig. 7a, were observed for both two phase liquid–gas and three phase flows. In the case of three phase flow, however, especially at high flow rates, the oil and water are somewhat mixed and the liquid phases appear "milky". The clear identification of two distinct liquid phases is difficult in these cases.

Fig. 7b illustrates three phase stratified and stratified wavy flows. For the downward stratified wavy flow, oil and water are well mixed and form a homogeneous dispersion (at high flow rates of $Q_O = 40\ m^3/h$, $Q_W = 40\ m^3/h$). The flow pattern in this case closely resembles a two phase stratified wavy flow except that the liquid phase is a non-transparent dispersion/emulsion. This three phase flow can probably be modeled as a two phase flow, though the properties of the phases may differ from the properties of the pure components. Another interesting observation for three phase flow is that, even for a horizontal three phase stratified flow as shown in Fig. 7b, some oil penetrates into the water phase at the bottom of the pipe and some water is entrained into the oil phase. This three phase stratified flow therefore differs from the simpler case (Lee, 1993) in which the three pure phases appear as three distinct layers, for which the stratified three phase flow model of Taitel et al. (1995) can be applied. The significant mixing of the oil and water may be due in part to the fact that the oil used in the experiments is kerosene, with properties relatively close to those of water.

Figs. 8 and 9 show the observed water–gas and oil–water–gas flow patterns, respectively, for all of the experiments. For two phase flow, at vertical and $\theta = 5°$, only bubble and elongated bubble flows were observed. The pipe deviation can be seen to affect the bubble/elongated bubble flow pattern transition only slightly between $\theta = 0°$ and $\theta = 5°$. The curve in the $\theta = 0°$ subplot is the transition line from so called bubbly to churn slug flow for water–air in a 20 cm diameter vertical pipe, observed by Ohnuki and Akimoto (2000). It can be seen that this curve closely matches the flow pattern transition from bubble to elongated bubble flow in this study. It should be noted that in our experiments, the elongated bubble flows observed for vertical and $\theta = 5°$ are different from those traditionally observed in small diameter pipes. They are more like the churn slug identified by Ohnuki and Akimoto (2000), where the large bubbles are not Taylor bubbles, but of irregular shape.

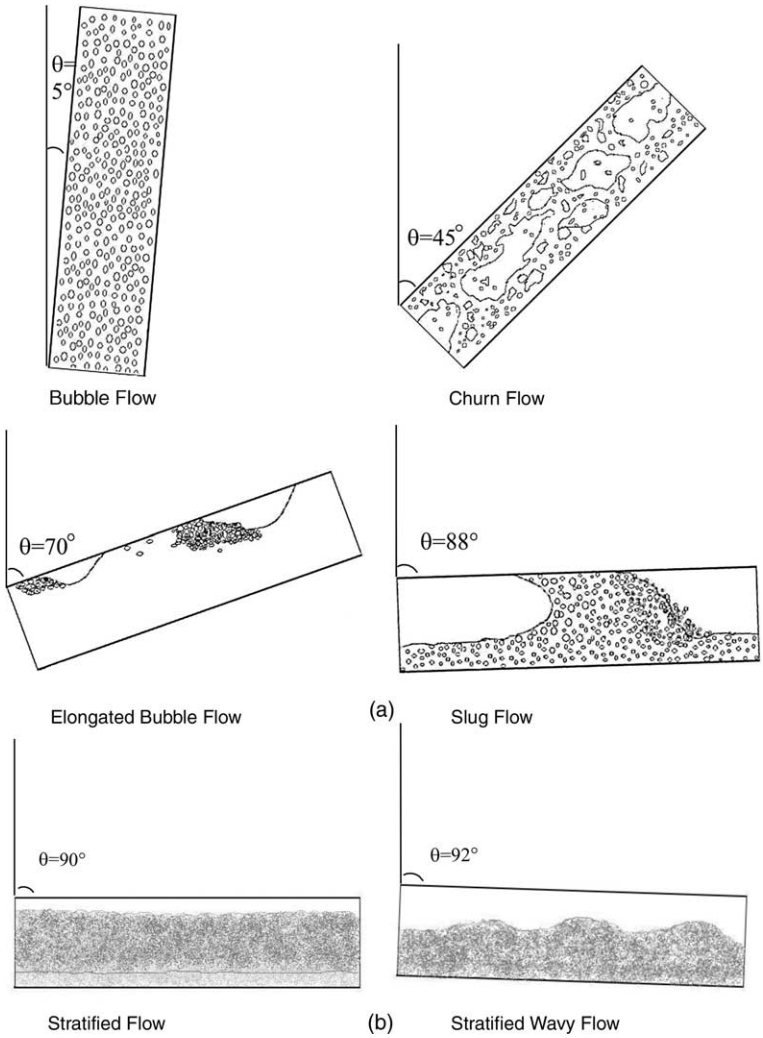

Fig. 7. (a) Sketch of some observed water–gas flow patterns with typical corresponding inclinations; (b) sketch of some observed oil–water–gas flow patterns with typical corresponding inclinations.

At 45°, most of the tests showed elongated bubble flow, though slug, bubble, and churn flows were also observed. From $\theta = 70°$ to 88°, only slug and elongated bubble flows were observed. For horizontal flow, the flow patterns were stratified or stratified wavy, except in one case where slug flow was observed at the highest water and gas flow rates investigated. Flows were all stratified for the downward inclination ($\theta = 92°$).

Similar observations can be made for the three phase flows in Fig. 9, though the precise locations of the flow transitions do change. For example, at $\theta = 45°$, the transition to slug flow occurs at lower V_{SG} in the case of three phase flow than for two phase flow. The water–gas and oil–water–gas flow patterns will be discussed further when the experimental observations are compared with predictions from a mechanistic model.

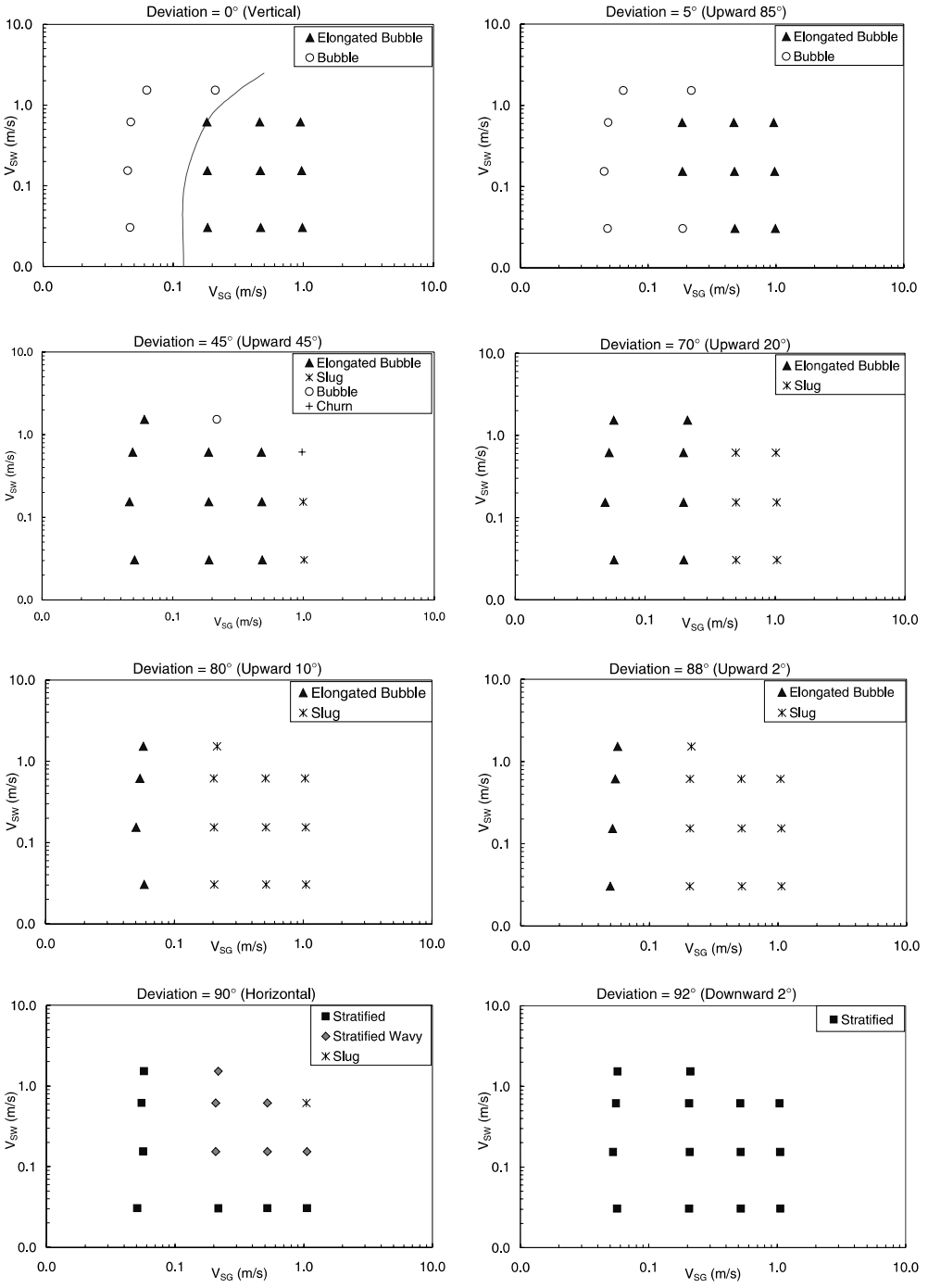

Fig. 8. Flow patterns for water–gas two phase flow.

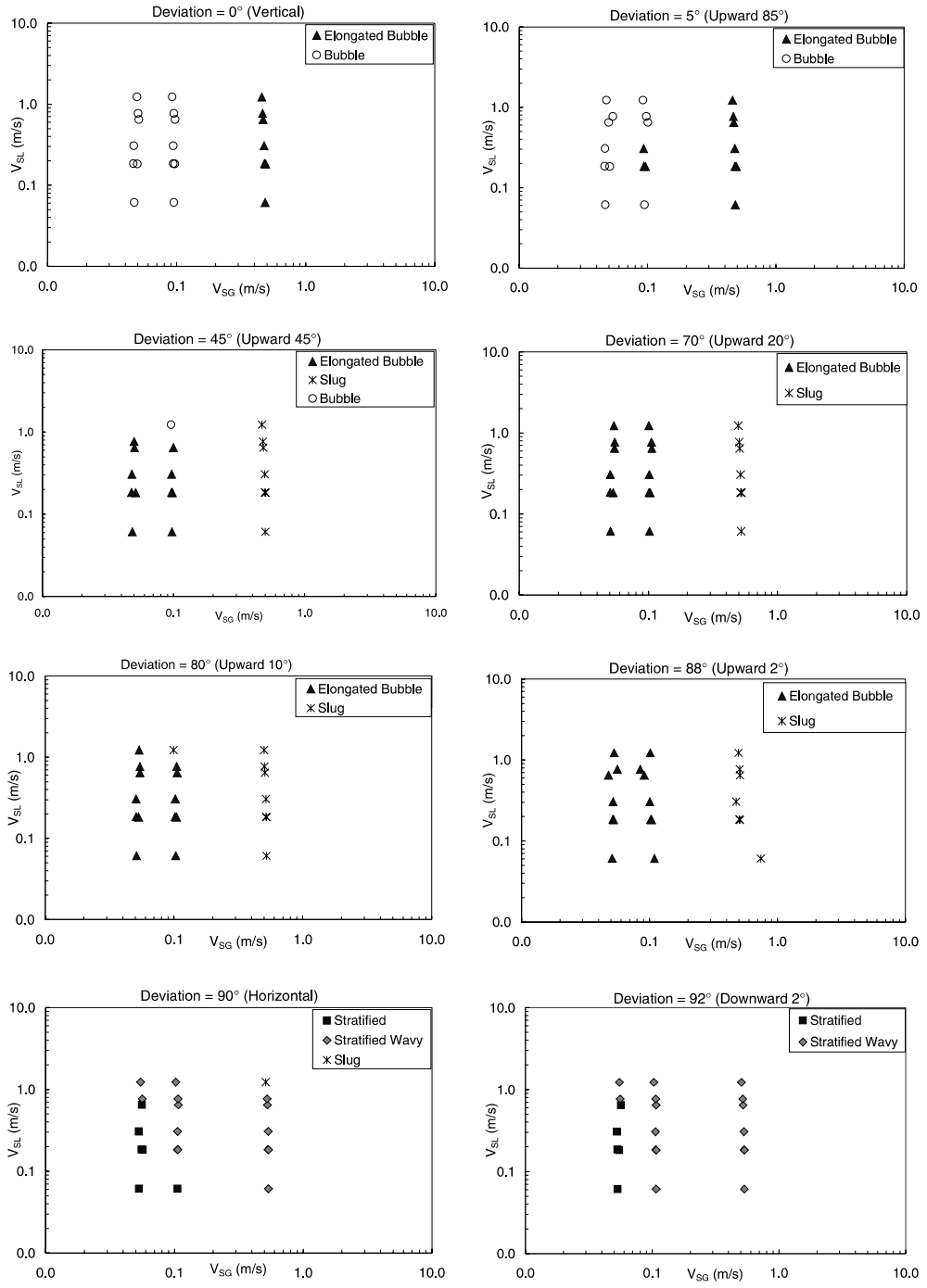

Fig. 9. Flow patterns for oil–water–gas three phase flow.

The observed oil–water flow patterns, classified according to the definitions of Oglesby (1979), are shown in Fig. 10. Segregated, semi-segregated, semi-mixed, mixed, dispersed, and homogeneous flow patterns were observed. Shi et al. (1999) also observed these six flow patterns for oil–water flows in a 10 cm pipe. The segregated flow regime occurs when the liquids flow in two distinct layers, with no mixing at the interface. As the mixture velocity is increased, some mixing occurs at the interface, and the flow becomes semi-segregated. The flow is said to be semi-mixed when fluids flow in three segregated layers, with a dispersion in the middle and two pure phases at the top (oil) and the bottom (water). Flow is also referred to as semi-mixed when it is segregated into a dispersion and a pure phase, with the dispersion volume less than half of the total pipe volume. Mixed flow occurs when the oil–water dispersion occupies more than half the pipe volume. When oil and water are totally mixed the flow pattern is referred to as dispersed (though concentration gradients may persist). At high mixture velocity, oil and water flow as a homogeneous phase without appreciable variation in concentration across the pipe diameter.

It is seen that for $0 \leqslant \theta \leqslant 45°$, only dispersed and homogeneous flows were observed, indicating that oil and water mix relatively easily at these deviations. In addition, the flow pattern map changes very little over $0 \leqslant \theta \leqslant 45°$. As the pipe deviates further, oil and water tend to become stratified, with two semi-mixed flows observed at low oil and water flow rates for $\theta = 70°$. As the pipe approaches horizontal, most of the flow patterns, including segregated, semi-segregated, semi-mixed, mixed, dispersed, and homogeneous, were observed. For downward flow ($\theta = 92°$), most flows were stratified, with only one dispersed flow observed at high oil and water flow rates.

5.2. Holdup

As discussed above, three major techniques were employed to measure steady-state holdup: shut-in, probe and nuclear (gamma densitometer) measurements. In order to gauge the accuracy and consistency between these various measurement techniques, we now compare and assess the results for holdup.

5.2.1. Shut-in holdup

The use of shut-in to measure steady-state holdup is a classic method and is considered to be one of the most reliable ways to measure holdup in multiphase flow systems. In order to correctly measure the steady-state holdup, the shut-in zone is usually confined to a section that has a fully developed flow with minimum inlet and outlet effects. In our experiments, the shut-in zone includes the entire test section; i.e., the full pipe length between the inlet and the outlet. This shut-in design is well-suited for the study of transient flow, though this approach introduces entrance and outlet effects into the shut-in holdup measurements. To gauge the magnitude of these effects, we compare the shut-in holdup with the other two holdup measurements. In addition, we use the probe measurements to estimate the magnitude of the inlet and outlet effects on the shut-in holdup.

5.2.2. Probe holdup

The probes detect the instantaneous fraction of water along the pipe diameter and can therefore be used to estimate holdup. Time-averaging of the probe data during the steady-state period gives an estimate of the holdup profile in the axial direction. Fig. 11a displays time-averaged results of

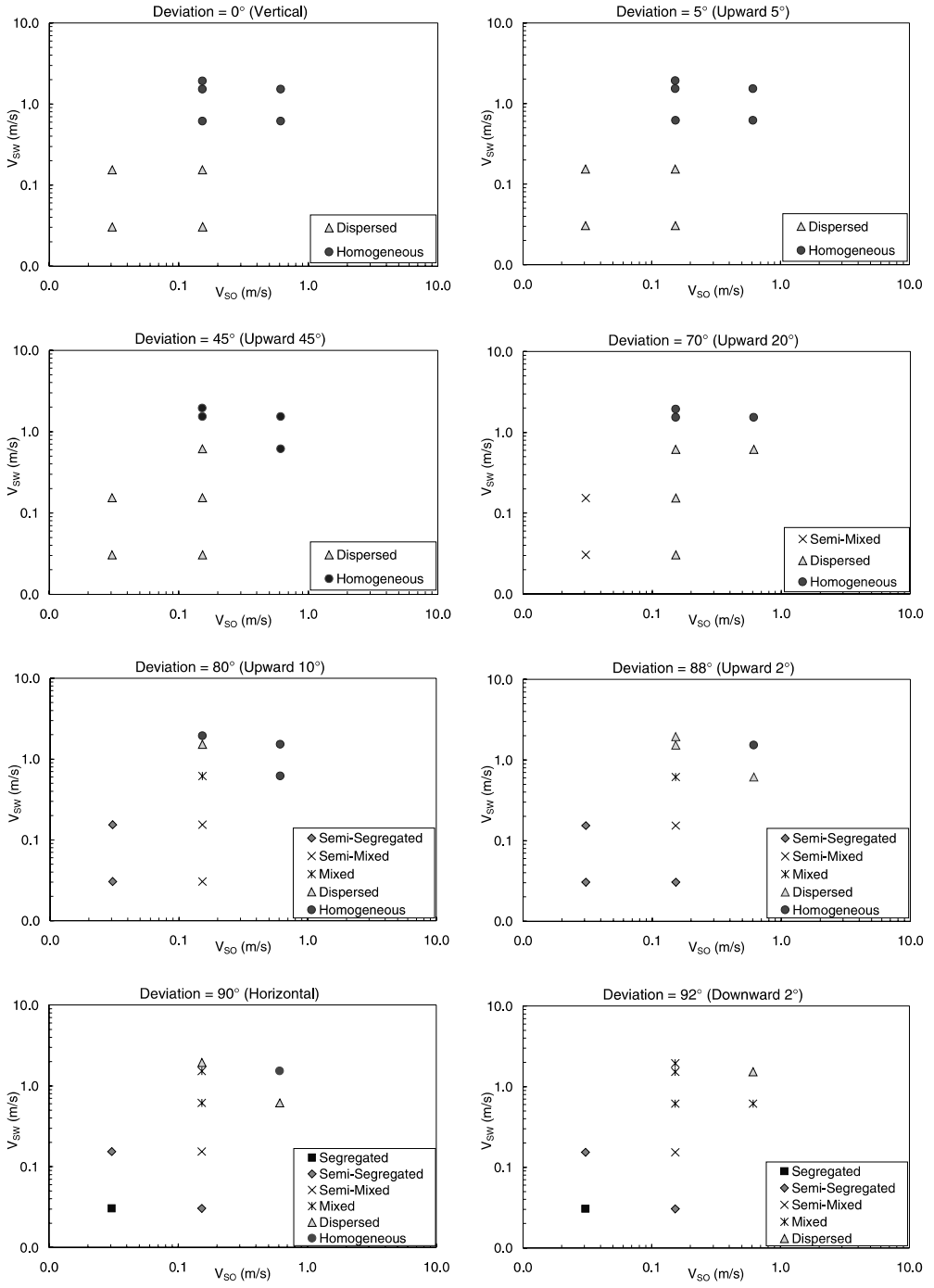

Fig. 10. Flow patterns for oil–water two phase flow.

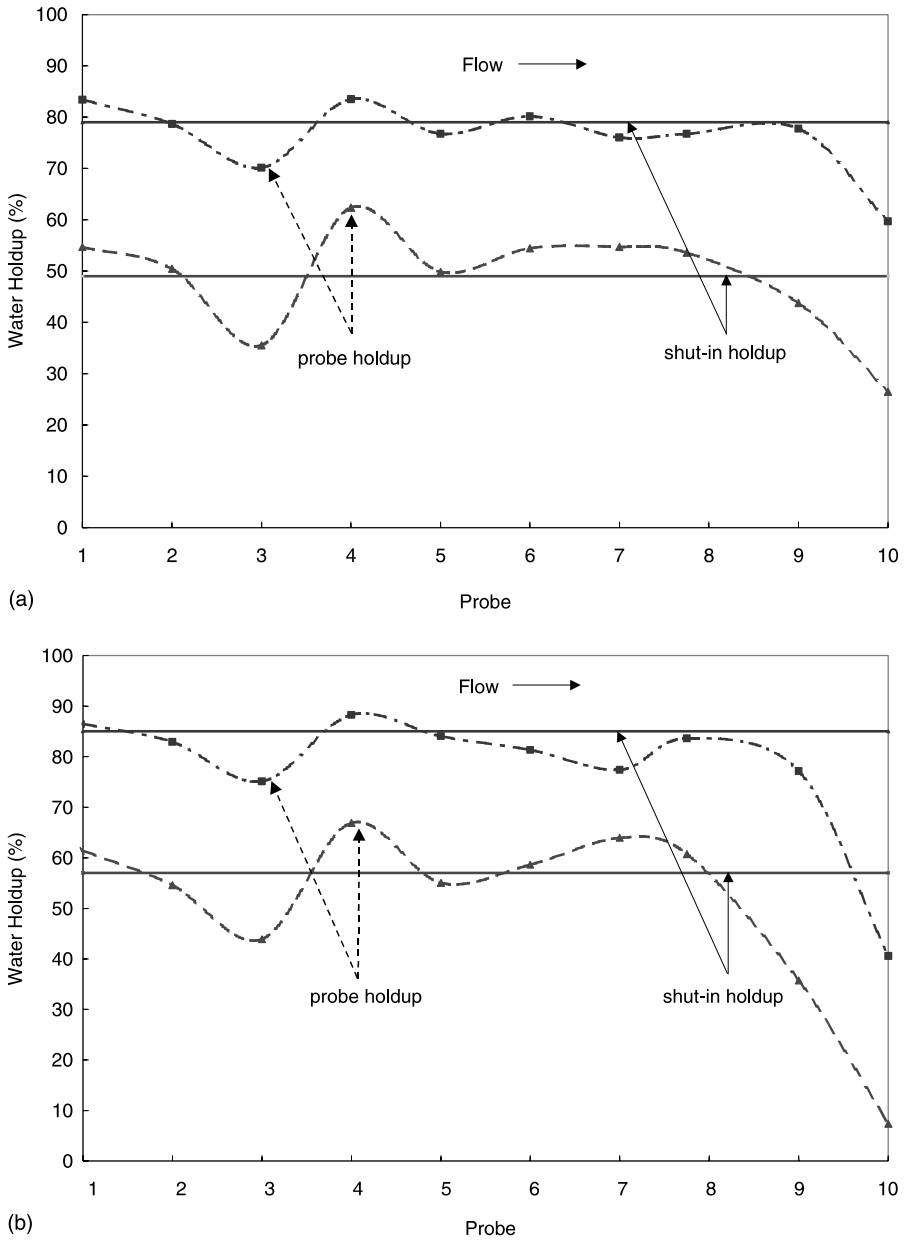

Fig. 11. (a) Comparison of shut-in and probe water holdup (upper curve for $\theta = 0°$, $Q_W = 40.5$ m^3/h, $Q_G = 28.2$ m^3/h, $H_W = 79\%$; lower curve for $\theta = 0°$, $Q_W = 2.0$ m^3/h, $Q_G = 60.2$ m^3/h, $H_W = 49\%$); (b) comparison of shut-in and probe water holdup (upper curve for $\theta = 45°$, $Q_O = 10.0$ m^3/h, $Q_W = 40.5$ m^3/h, $H_W = 85\%$; lower curve for $\theta = 70°$, $Q_O = 10.0$ m^3/h, $Q_W = 10.1$ m^3/h, $Q_G = 6.2$ m^3/h, $H_W = 57\%$).

probe holdup for vertical water–gas systems; Fig. 11b shows analogous results for inclined oil–water and oil–water–gas systems. The curves depict the probe holdup measurements while the corresponding horizontal lines display the shut-in holdup values. From the figures, we see that the

general agreement between the time-averaged probe holdup and the shut-in holdup is reasonable except near the outlet (probe 10 and in some cases probe 9), where a consistent end effect is evident. Away from the outlet, the probe holdup does display some variation along the pipe, though this variation is relatively small compared to the end effect. In addition, the inlet effect appears to be of about the same magnitude as the variation along the pipe. As was evident in Figs. 3–6, probes 3 and 4 show systematic variation from the shut-in holdup.

The results of Fig. 11a and b do indicate, however, that most of the time-averaged probe data (except for the end effect) are of reasonable accuracy; e.g., about ±20%. The probe data are not as accurate as the shut-in or nuclear measurements. These data will therefore not be used to compute steady-state holdup, though they will be used in subsequent work to evaluate and model the transient behavior of the system.

Although the probe data do not provide the most accurate results for steady-state holdup, we can use the probe data to estimate the magnitude of the outlet effect on the shut-in holdup measurements. To accomplish this, we express the shut-in holdup as the weighted sum of the "stabilized" holdup H_W^{stab} (i.e., the holdup over the portion of the pipe not impacted by the end effect, corresponding to the zone instrumented with probes 1–8) and the "end effect" holdup H_W^{end} (as measured by probes 9 and 10) as follows:

$$H_W^{si} = l_s H_W^{stab} + l_e H_W^{end} = l_s H_W^{stab} + l_e \left(\frac{H_W^{end}}{H_W^{stab}} \right) H_W^{stab}, \tag{5}$$

where H_W^{si} is the shut-in holdup, l_s is the fractional length of the pipe over which the flow is stabilized (here $l_s \approx 0.8$) and l_e is the fractional length of the pipe over which the end effect acts ($l_e \approx 0.2$). We write Eq. (5) in terms of (H_W^{end}/H_W^{stab}), which we designate as R, because this quantity can be estimated from the probe data. Rearranging Eq. (5), we now have

$$H_W^{stab} = \frac{H_W^{si}}{l_s + l_e R}. \tag{6}$$

The quantity $F = (l_s + l_e R)^{-1}$ provides the relationship between the measured shut-in holdup H_W^{si} and the stabilized holdup H_W^{stab}. We compute this quantity from the probe data for the three different fluid systems at different inclinations. The results are reported in Table 2. Each entry in the table represents the average value of F over all of the experiments in the designated range. Although there is a high degree of scatter in F between experiments, for inclinations other than 92° the data show similar averages and scatter, with the exception of horizontal flows for $H_W < 40\%$, for which F is larger (e.g., $F \approx 1.09$ for water–gas flows in this range). From the table,

Table 2
Ratio of stabilized holdup to shut-in holdup

	Inclination from vertical	
	$\theta = 92°$	$0° \leqslant \theta \leqslant 90°$
Water–gas	1.16	1.04
Oil–water	1.09	1.06
Oil–water–gas	1.16	1.08

we see that the end effect for most flows ($\theta \neq 92°$) causes the stabilized holdup to deviate from the shut-in holdup by about a factor of 1.04–1.08.

5.2.3. Nuclear holdup

The nuclear (gamma) densitometer measurement offers another useful way to determine holdup. The densitometer is located between probes 7 and 8 (see Fig. 2), so the nuclear data should not be influenced by the end effect. The data must be interpreted in terms of homogeneous, stratified or pure slug flow (see Eqs. (2)–(4) above). The fact that the flow is generally not exactly one of these idealized cases will introduce some error into the holdup predictions, which we now discuss.

Fig. 12a and b show cross-plots of the mean density derived from the shut-in and nuclear data for all of the experiments. In these and subsequent plots we do not modify the shut-in holdup data to account for the end effect because this correction is variable between experiments and was shown above to be relatively small on average. The flow was assumed homogeneous in Fig. 12a in the interpretation of the gamma densitometer data. As we can see from this figure, the agreement is good for the higher density tests. For flows with densities greater than 800 kg/m^3 the agreement between the nuclear and shut-in densities is very close, with only a few of the data points falling outside of $\pm 10\%$. For densities in the range 500 kg/m^3–800 kg/m^3, most of the data agree to within $\pm 20\%$. There is, however, a systematic offset for tests where the mean density is less than about 400 kg/m^3. Inspection of the video shows that all of these experiments display some degree of stratification.

The nuclear data is reinterpreted in terms of stratified flow in Fig. 12b. It can be seen that for densities less than 400 kg/m^3 the agreement between shut-in and nuclear results is improved, though errors do persist. In both cases, the results for the flows with densities greater than 800 kg/m^3 are quite satisfactory. Most of the outliers fall in the lower density range. The lower density data correspond to cases for which end effects are significant ($\theta = 92°$ and $\theta = 90°$ with $H_W < 40\%$), so we expect to observe some discrepancies in this range. Issues such as the intermittency of the flow and backflow behind slugs may also complicate the data interpretation.

From the discussion above and that in Section 2.3, it is apparent that the interpretation of the nuclear densitometer data can introduce some uncertainty into the density and holdup predictions. In Fig. 13a we quantify this uncertainty for water–gas flows. Specifically, for a given nuclear count, we compute holdup using each of Eqs. (2)–(4). This provides some indication of the potential error in the H_W derived from the nuclear measurements. From the figure we see that the maximum difference between the largest and smallest estimates for H_W is about 14% in absolute terms.

In Fig. 13b we cross plot the nuclear holdup data against the shut-in holdup for water–gas flow. The nuclear data here are plotted as "bars" rather than points, with the minimum and maximum values of each bar determined from Fig. 13a. Note that the data for shut-in holdup less than 40% are significantly influenced by the end effect. If we accounted for the end effect, these data bars would be shifted to the right by about a factor of 1.09 or more, which would bring them closer to the 45° line. It can be seen from the figure that the shut-in and nuclear holdup data are in quite reasonable agreement, particularly at higher values of water holdup.

Fig. 14a and b show the shut-in and the nuclear water holdup results for water–gas and oil–water systems, and liquid holdup for oil–water–gas systems. Here we show results only under the assumptions of homogeneous and stratified flows. We do not interpret the data under the pure

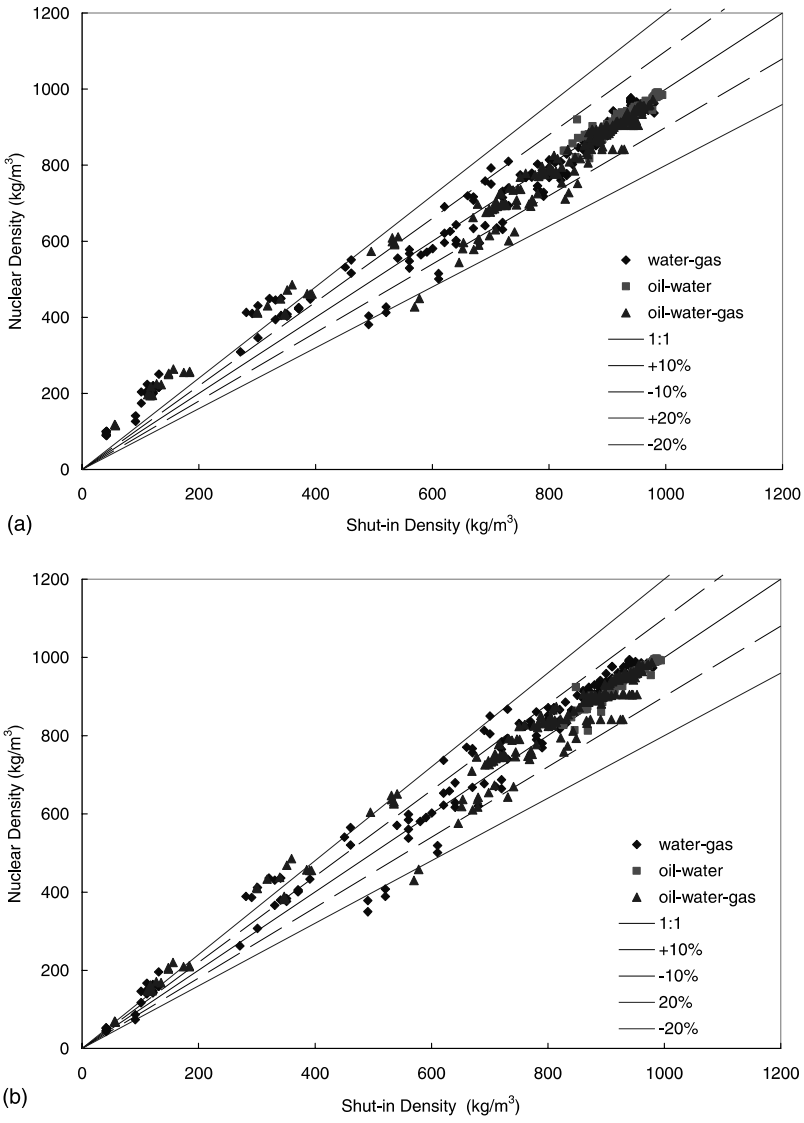

Fig. 12. (a) Comparison of shut-in and nuclear homogeneous density; (b) comparison of shut-in and nuclear stratified density.

slug flow assumption discussed above because it is not applicable to all of the fluid systems considered. From Fig. 14a and b, we see that the holdup computed from the gamma densitometer is in reasonably good agreement with the shut-in holdup for both two and three phase flows. More specifically, under the assumption of stratified flow in Fig. 14b, 93% of the data falls within the $\pm 20\%$ range and 84% of the data falls within the $\pm 10\%$ range. Comparing Fig. 14a and b, it can be seen that the results are slightly more accurate when the fluids are assumed to be stratified. This may be because (1) many of the flows display some degree of stratification and (2) for the flows that are more homogeneous, the calculation of holdup under the assumption of stratified flow

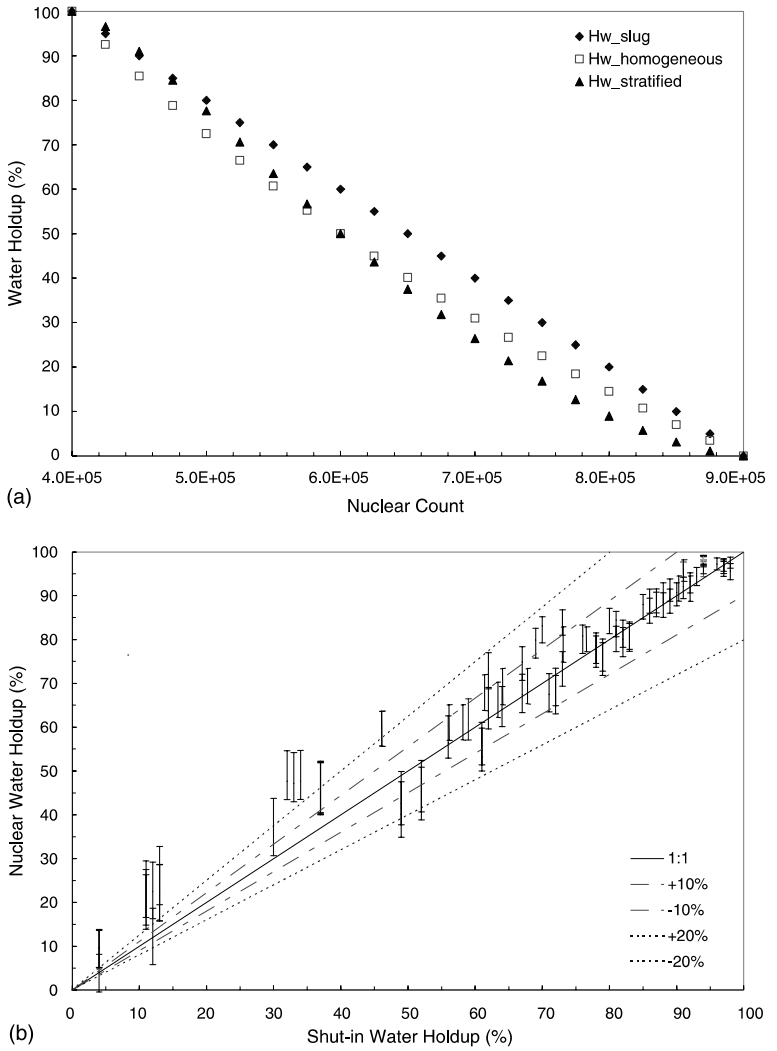

Fig. 13. (a) Range of nuclear water holdup under different flow assumptions; (b) comparison of shut-in and nuclear water holdup for water–gas flow.

does not induce much error. In any event, the general level of agreement between the nuclear and shut-in results suggests that both techniques are of reasonable accuracy for the measurement of holdup. This agreement further suggests that the inlet and outlet effects on the shut-in holdup are not significant in the majority of cases, as was also indicated by the probe data.

5.2.4. Steady-state holdup

From the discussion and results presented above, we conclude that two and three phase holdups can be assessed with reasonable accuracy via the shut-in holdup measurement. The

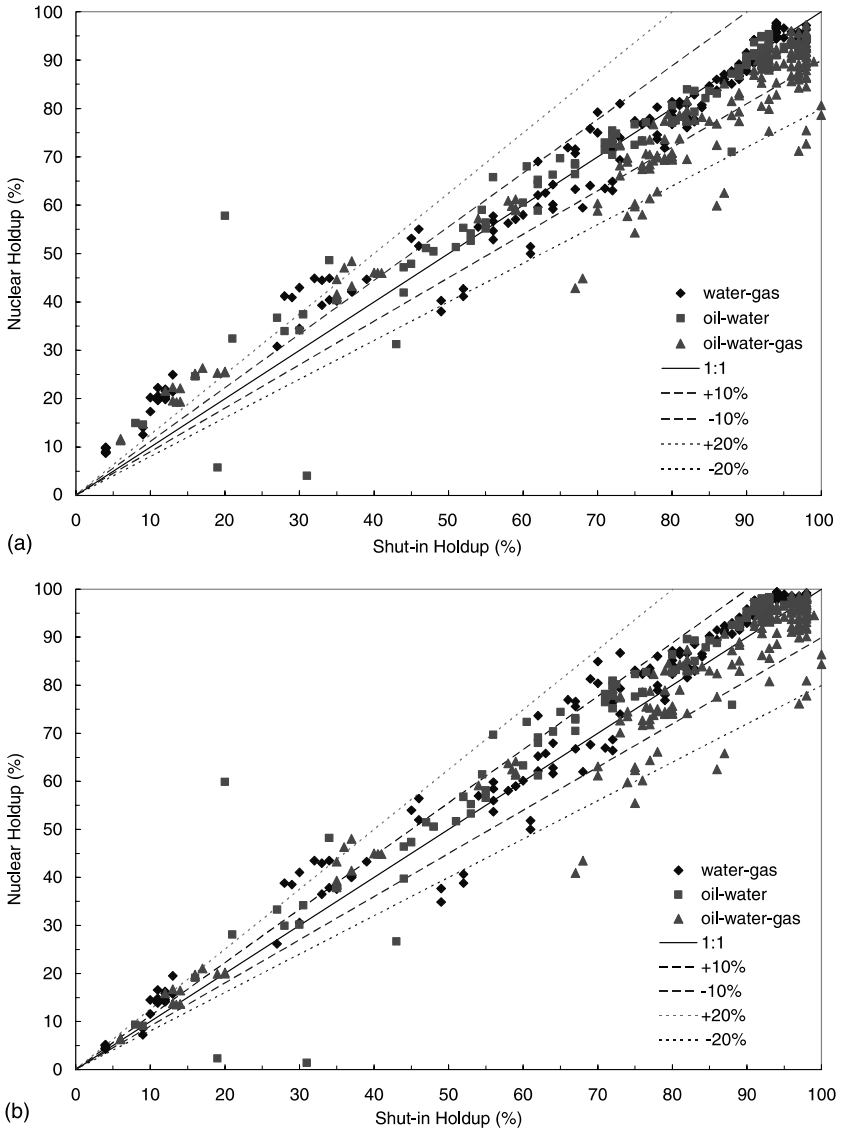

Fig. 14. (a) Comparison of shut-in and nuclear homogeneous liquid holdup; (b) comparison of shut-in and nuclear stratified liquid holdup.

shut-in measurement itself in this experiment is very accurate, with a measurement error of less than 1% for holdups of less than 94% (for holdup greater than 94%, the interface is not visible due to the metal sections of pipe near the outlet). Furthermore, the shut-in holdup is in generally good agreement with the nuclear measurements, confirming that the differences between the measured values of the steady-state holdup and the shut-in holdup are not large. The impact of the end effect was additionally shown to be small (8% or less) in most cases. Therefore, the shut-in holdup will be used to represent stabilized steady-state holdup. In the following discussion, we use 'holdup' to

mean shut-in water holdup for two phase flows and shut-in liquid (oil + water) holdup for three phase flows.

Figs. 15–17 show holdup versus input liquid cut (or non-slip holdup) for water–gas, oil–water–gas (oil and water are treated as one liquid phase), and oil–water flows, respectively. Input liquid cut (C_L) is simply defined as the inlet flowing fraction of water (for two phase flow) or inlet flowing fraction of total liquid (for three phase flows) and is given by $Q_W/(Q_W + Q_G)$, $Q_W/(Q_W + Q_O)$ or $(Q_O + Q_W)/(Q_O + Q_W + Q_G)$ for the three types of systems. The error bars indicated in the figures are ±5%, as determined from the repeated tests. Note that this error is comparable to the magnitude of the end effect (which would shift the data up by about 5%) as estimated from the probe data. We include data for the vertical case in all plots, as well as data at other inclinations. Here, we define the slippage in terms of the difference between the in situ liquid volume fraction (liquid holdup) and the input liquid volume fraction; i.e., $S = H_L - C_L$, where S is slippage. In the figures, the vertical distance from any point to the $H_L = C_L$ line gives the magnitude of slippage between the phases.

The results for water–gas flows at vertical and 70° deviation are shown in Fig. 15. It is seen that the slippage decreases as the flow rates increase for the same inlet flowing fractions. The slippage is lowest at the highest holdup values. The figure also shows the effect of deviation on slippage. In all cases there is more slippage for 70° deviation than for vertical flow, though the magnitude of the effect is not that significant.

Fig. 16 presents the liquid holdup for three phase systems, with oil and water treated as one liquid phase. These results are reasonably close to the results of the water–gas flow shown in Fig. 15 and display similar trends. This suggests that, at least in this case, oil and water can be considered as a single liquid phase for the calculation of liquid holdup. The plot also shows that at very high liquid holdup values, there is little slippage for either deviation.

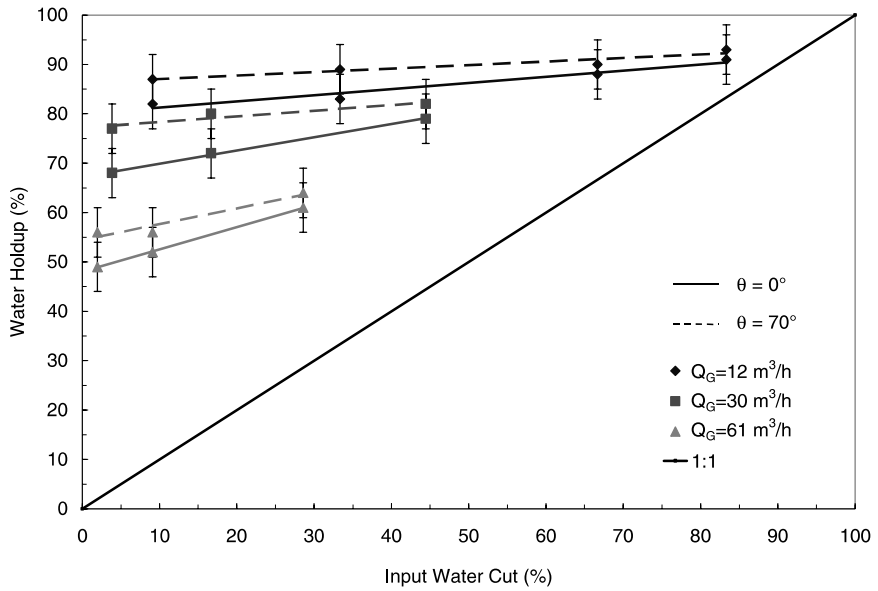

Fig. 15. Holdup for water–gas systems for $\theta = 0°$ and $\theta = 70°$.

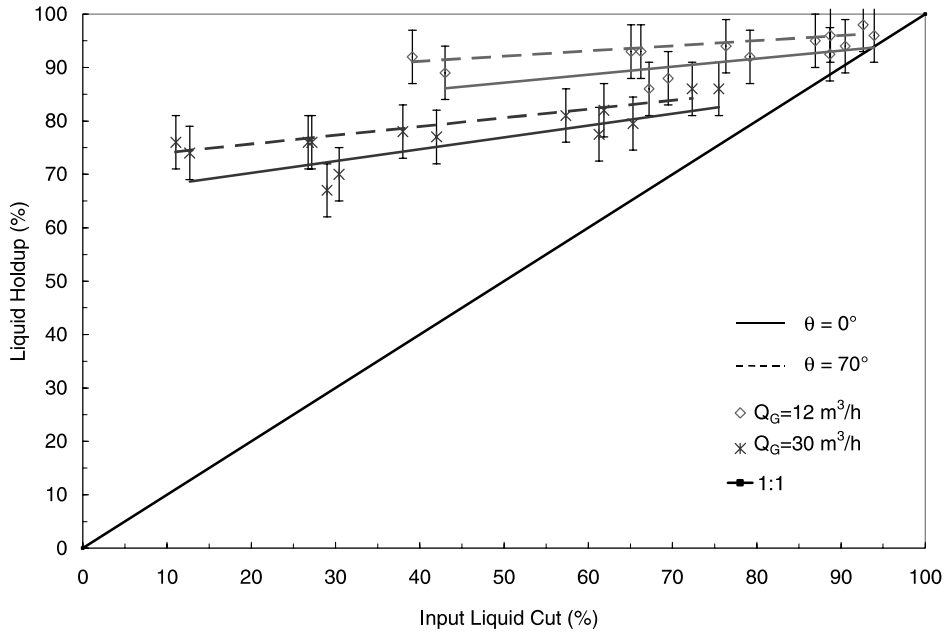

Fig. 16. Holdup for oil–water–gas systems for $\theta = 0°$ and $\theta = 70°$.

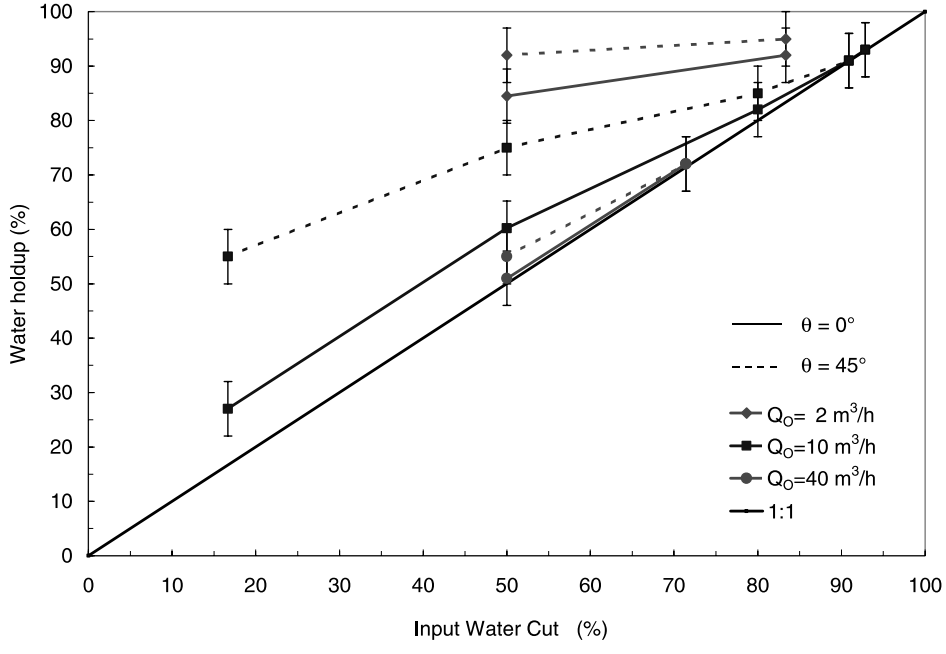

Fig. 17. Holdup for oil–water systems for $\theta = 0°$ and $\theta = 45°$.

Fig. 17 presents results for oil–water systems for vertical flow and flow at a 45° inclination. It is evident that at very low flow rates of both oil and water, the slippage is relatively high, though it is

still much less than that observed for liquid–gas systems. The results also show that, at low flow rates, the effect of pipe deviation is similar to that for liquid–gas flow. At the highest water and oil flow rates, however, there is very little slippage and deviation has a minimal effect. This is because, at high flow rates, oil and water are well mixed and form a homogeneous dispersion or emulsion (these experiments were in fact observed to be in homogeneous flow), and there is very little slip between the two phases for homogeneous flow at any deviation.

5.3. Comparison with mechanistic model

5.3.1. Flow pattern

We now compare the observed flow patterns with those predicted by a recent mechanistic model (Petalas and Aziz, 2000). The transition criteria in this model are based in part on the earlier work of Barnea (1987). The Petalas and Aziz (2000) model was developed using a large amount of data and was shown to provide more reliable predictions than some of the earlier mechanistic models (e.g., Xiao et al., 1990; Dukler et al., 1964).

The mechanistic model predicts the observed flow patterns of water–gas flows very reliably, as shown in Table 3. For example, for water–gas vertical flow, all five bubble flows are predicted correctly and only one of the nine elongated bubble flows was predicted to be bubble flow. For flows with more deviation from the vertical, the results are not as accurate but are still quite good. For example, at a 45° deviation, the model predicts all the tests to be elongated bubble flow, and thus does not predict the observed bubble, slug and churn flows. However, considering that elongated bubble, slug and churn flows can all be classified as intermittent flows, the model predictions are reasonable.

For three phase flow, with the oil–water–gas system treated as a liquid–gas system, similar accuracy in flow pattern prediction was obtained. A number of cases are presented in Table 4. For example, for horizontal flows, with stratified smooth and stratified wavy flows grouped together as stratified flows, the model predicts eight of the ten flow patterns correctly (one stratified wavy flow is predicted to be elongated bubble flow, and one slug flow is predicted to be stratified wavy flow). Similar levels of accuracy are also observed for most of the other three phase flow data.

The relatively high degree of accuracy of the Petalas and Aziz (2000) mechanistic model is somewhat surprising, as the model was developed based largely on experimental results for small diameter ($< \sim 5$ cm) pipes. This suggests that these data, and the approximate models built into the mechanistic description, are generally adequate for the purposes of determining flow pattern in the parameter range considered here. As we shall see below, this model is also able to provide somewhat reasonable predictions for holdup, though the accuracy is not as good as for the prediction of flow pattern.

5.3.2. Steady-state holdup

Fig. 18 presents detailed results for water–gas flows at a number of pipe deviations (vertical to 2° above horizontal). As discussed previously, the measured holdup data for downward and some of the horizontal flows are considered to be less reliable and are therefore not shown here. Holdup predicted from the mechanistic model is plotted against the experimental shut-in values, with the data symbol indicating pipe deviation. The mechanistic model provides reasonable estimates for

Table 3
Comparison of experimental and predicted water–gas flow patterns

Q_W (m^3/h)	Q_G (m^3/h)	Deviation from vertical							
		88°		70°		45°		0°	
		Exp	Predict	Exp	Predict	Exp	Predict	Exp	Predict
2	5	EB	EB	EB	EB	EB	EB	B	B
10	5	EB	EB	EB	EB	EB	EB	B	B
40	5	EB	EB	EB	EB	EB	EB	B	B
100	5	EB	EB	EB	EB	EB	EB	B	B
2	20	Slug	EB	EB	EB	EB	EB	EB	EB
10	20	Slug	EB	EB	EB	EB	EB	EB	EB
40	20	Slug	EB	EB	EB	EB	EB	EB	B
100	20	Slug	EB	EB	EB	B	EB	B	B
2	50	Slug	EB	Slug	EB	EB	EB	EB	EB
10	50	Slug	EB	Slug	EB	EB	EB	EB	EB
40	50	Slug	EB	Slug	EB	EB	EB	EB	EB
2	100	Slug	EB	Slug	EB	Slug	EB	EB	EB
10	100	Slug	EB	Slug	EB	Slug	EB	EB	EB
40	100	Slug	Slug	Slug	Slug	Churn	EB	EB	EB

Key: Exp = experimental; Predict = predicted; EB = elongated bubble; B = bubble.

Table 4
Comparison of experimental and predicted oil–water–gas flow patterns

Q_W (m^3/h)	Q_O (m^3/h)	Q_G (m^3/h)	Deviation from vertical					
			90°		70°		5°	
			Exp	Predict	Exp	Predict	Exp	Predict
2	2	5	StratS	StratS	EB	EB	B	B
10	10	5	StratS	StratS	EB	EB	B	B
2	2	10	StratS	StratS	EB	EB	B	EB
10	10	10	StratW	StratS	EB	EB	EB	B
40	10	10	StratW	StratW	EB	EB	B	B
40	40	10	StratW	EB	EB	EB	B	B
2	2	50	StratW	StratS	Slug	EB	EB	EB
10	10	50	StratW	StratW	Slug	EB	EB	EB
40	10	50	StratW	StratW	Slug	EB	EB	EB
40	40	50	Slug	StratW	Slug	Slug	EB	B

Key: Exp = experimental; Predict = predicted; StratS = stratified smooth; StratW = stratified wavy; EB = elongated bubble; B = bubble.

holdup for much of the data, though there is a clear tendency toward underprediction by the model. The accuracy of the model appears to improve slightly as the pipe orientation approaches horizontal.

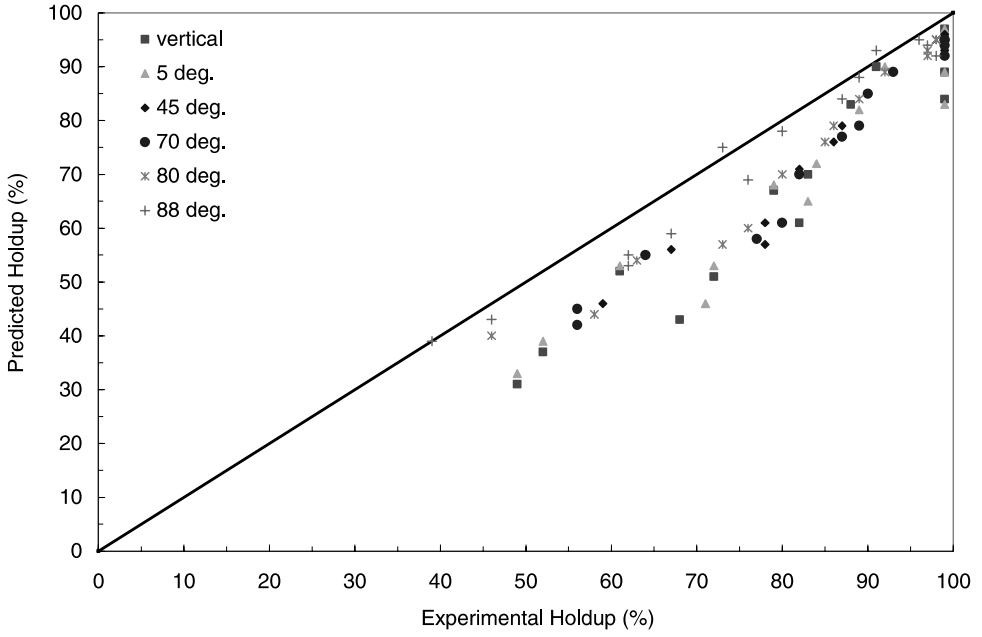

Fig. 18. Predicted water holdup for water–gas systems ($0° \leqslant \theta \leqslant 88°$).

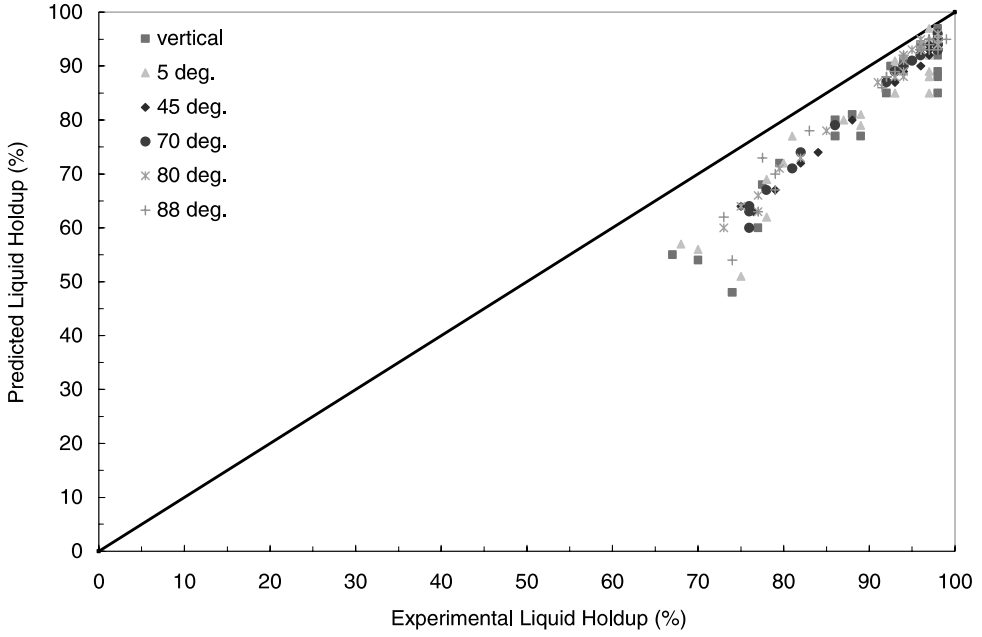

Fig. 19. Predicted liquid holdup for oil–water–gas systems ($0° \leqslant \theta \leqslant 88°$).

Fig. 19 displays predicted versus experimental results for liquid holdup in three phase systems at pipe deviations from vertical to 2° above horizontal. The quality of the mechanistic model

appears almost as good in this case as in the case of two phase flow at these inclinations (see Fig. 18). As was also the case for two phase flow, the model appears to be slightly more accurate as the deviation from vertical increases. Fig. 19 also shows that predictions from the Petalas and Aziz (2000) mechanistic model are better at high liquid holdup than at lower liquid holdup. At the high liquid flow rates corresponding to these data, there is little slippage between oil and water. This is consistent with the assumptions of the mechanistic model, which treats oil and water as a single liquid phase, and thus neglects slippage between the oil and water phases. Taken in total, the results presented in Figs. 18 and 19 indicate that the existing mechanistic model is able to provide somewhat reasonable estimates of water holdup (in two phase systems) and liquid holdup (in three phase systems), though the predictions could still be improved.

6. Conclusions

The following main conclusions can be drawn from this experimental study.

- A large scale, well-instrumented apparatus was designed, built and tested for the study of steady-state and transient multiphase flow in large diameter, inclined pipes.
- Unique holdup data were obtained for steady-state and transient flows. Water–gas, oil–water and oil–water–gas systems were studied. The effects of the flow rates of the different phases and pipe deviation on holdup were evaluated.
- Steady-state holdups from nuclear measurements were in reasonably close agreement with absolute shut-in measurements. Probe data can provide transient and steady-state holdup profiles along the length of the pipe, though the accuracy of the probes was not as high as that of the nuclear densitometer or shut-in measurements.
- Detailed flow pattern maps were generated over the entire range of flow rates and pipe inclinations for all of the fluid systems. The maps for the water–gas and oil–water–gas systems were found to be qualitatively similar.
- The Petalas and Aziz (2000) mechanistic model was able to predict the experimentally observed flow pattern with high accuracy and holdup with reasonable accuracy.

Acknowledgements

We are grateful to Schlumberger for supporting this work. We thank A. von Hirschberg, an intern at Schlumberger, for his assistance in building the experimental equipment and with some of the measurements. The Stanford University group was funded in part by the industrial affiliates of the Stanford Project on the Productivity and Injectivity of Horizontal Wells (SUPRI-HW).

References

Açikgöz, M., Franca, L., Lahey, R.T., 1992. An experimental study of three-phase flow regimes. Int. J. Multiphase Flow 18, 327–336.

Angeli, P., Hewitt, G.F., 1998. Pressure gradient in horizontal liquid–liquid flows. Int. J. Multiphase Flow 24, 1183–1203.

Arirachakaran, S., Oglesby, K.D., Malinovsky, M.S., Shoham, O., Brill, J.P., 1989. An analysis of oil–water flow phenomena in horizontal pipes, SPE Paper 18836.

Barnea, D., 1987. A unified model for predicting flow pattern transitions for the whole range of pipe inclinations. Int. J. Multiphase Flow 13, 1–12.

Beggs, H.D., 1972. An experimental study of two-phase flow in inclined pipes. Ph.D. Dissertation, University of Tulsa, OK.

Beggs, H.D., Brill, J.P., 1973. A study of two-phase flow in inclined pipes. J. Pet. Technol. (May), 607–617.

Cheng, H., Hills, J.H., Azzorpardi, B.J., 2000. A study of the bubble-to-slug transition in vertical gas–liquid flow in columns of different diameter. Int. J. Multiphase Flow 24, 431–452.

Dikken, B.J., 1990. Pressure drop in horizontal wells and its effects on production performance. J. Pet. Technol. 42, 1426–1433.

Dukler, A.E., Wicks, M., Cleveland, R.G., 1964. Fractional pressure drop in two phase flow: A. A comparison of existing correlations for pressure loss and holdup. AIChE J. 10, 38–45.

Flores, J.G., Sarica, C., Chen, T.X., Brill, J.P., 1997. Investigation of holdup and pressure drop behavior for oil–water flow in vertical and deviated wells. ETCE-98, Paper no. 10797.

Gopal, M., Jepson, W.P., 1997. Development of digital image analysis techniques for the study of velocity and void profiles in slug flow. Int. J. Multiphase Flow 23, 945–965.

Hasan, A.R., Kabir, C.S., 1988. Predicting multiphase flow behavior in a deviated well. SPE Prod. Eng. 3, 474–482.

Holmes, J.A., Barkve, T., Lund, Ø., 1998. Application of a multi-segment well model to simulate flow in advanced wells. SPE Paper 50646.

Jepson, W.P., Taylor, R.E., 1993. Slug flow and its transitions in large-diameter horizontal pipes. Int. J. Multiphase Flow 19, 411–420.

Lahey, R.T., Açikgöz, M., Franca, L., 1992. Global volumetric phase fractions in horizontal three-phase flows. AIChE J. 38, 1049–1058.

Lee, A.H., 1993. A study of flow regime transitions for oil–water–gas mixture in large diameter horizontal pipelines. MS. Thesis, Ohio University, OH.

Oglesby, K.D., 1979. An experimental study on the effects of oil viscosity, mixture velocity and water fraction on horizontal oil–water flow. MS. Thesis, University of Tulsa, OK.

Ohnuki, A., Akimoto, H., 2000. Experimental study on transition of flow pattern and phase distribution in upward air–water two-phase flow along a large vertical pipe. Int. J. Multiphase Flow 26, 367–386.

Ouyang, L.B., Petalas, N., Arbabi, S., Schroeder, D.E., Aziz, K., 1998. An experimental study of single-phase and two-phase fluid flow in horizontal wells. SPE Paper 46221.

Pal, R., 1993. Pipeline flow of unstable and surfactant-stabilized emulsions. AIChE J. 39, 1754–1764.

Petalas, N., Aziz, K., 2000. A mechanistic model for multiphase flow in pipe. J. Can. Pet. Technol. 39, 43–55.

Scott, S.L., Shoham, O., Brill, J.P., 1989. Prediction of slug length in horizontal, large-diameter pipes. SPE Prod. Eng., 335–340.

Shi, H., 2001. A study of oil–water flows in large diameter horizontal pipelines. Ph.D. Dissertation, Ohio University, OH.

Shi, H., Cai, J.Y., Jepson, W.P., 1999. The effect of surfactants on flow characteristics in oil/water flows in large diameter horizontal pipelines. Multiphase 99, 181–199.

Taitel, Y., Barnea, D., Brill, J.P., 1995. Stratified three phase flow in pipes. Int. J. Multiphase Flow 21, 53–60.

Tshuva, M., Barnea, D., Taitel, Y., 1999. Two-phase flow in inclined parallel pipes. Int. J. Multiphase Flow 25, 1491–1503.

Vedapuri, D., 1999. Study on oil–water flows in inclined pipelines. MS. Thesis, Ohio University, OH.

Wilkens, R.J., 1997. Prediction of the flow regime transitions in high pressure, large diameter inclined multiphase pipelines. Ph.D. Dissertation, Ohio University, OH.

Woods, B.D., Hurburt, E.T., Hanratty, T.J., 2000. Mechanism of slug formation in downwardly inclined pipes. Int. J. Multiphase Flow 21, 977–998.

Wu, H., Zhou, F., Wu, Y., 2001. Intelligent identification system of flow regime of oil–gas–water multiphase flow. Int. J. Multiphase Flow 27, 459–475.

Xiao, J.J., Shoham, O., Brill, J.P., 1990. A comprehensive mechanistic model for two-phase flow in pipelines. SPE Paper 20631.